Dynamic light experiments and semi-automated plant phenotyping enabled by self-built growth racks and simple upgrades to the IMAGING-PAM

Dominik Schneider[a↓], Laura S. Lopez[b↓], Meng Li[a], Joseph D. Crawford[b], Helmut Kirchhoff[a] and Hans-Henning Kunz[b]*

[a] Institute of Biological Chemistry, Washington State University, PO Box 646340, Pullman, WA, 99164-6340, USA

[b] Plant Physiology, School of Biological Sciences, Washington State University, PO Box 644236, Pullman, WA 99164-4236, USA

[↓]both authors contributed equally

*Corresponding authors: Hans-Henning Kunz, henning.kunz@wsu.edu +1 (509) 335-7698

Orchid IDs: 0000-0002-5846-5033 (D.S.), 0000-0003-4038-9199 (L.S.L.), 0000-0001-9831-8575 (M.L.), 0000-0001-8754-6599 (J.D.C), 0000-0001-5874-3681 (H.K.), 0000-0001-8000-0817 (H.-H.K.)

Abstract

Background: Over the last years, several plant science labs have started to employ fluctuating growth light conditions to simulate natural light regimes more closely. Under fluctuating light, many plant mutants previously described as phenotype-free under standard constant light have started to reveal quantifiable effects. Moreover, many subtle plant phenotypes become intensified and thus can be studied in more detail. This observation has caused a paradigm shift within the photosynthesis research community and an increasing number of scientists are interested in using dynamic growth light conditions. However, high installation costs for controllable LED setups as well as costly phenotyping equipment make it hard for small academic groups to compete in this emerging field.

Results: We show a simple do-it-yourself approach using off-the-shelf parts to enable dynamic light growth experiments. Our results using previously published fluctuating light sensitive mutants, *stn7* and *pgr5,* confirm that our low-cost setup yields similar results as top-prized commercial growth regimes. Moreover, we show how to reconfigure a standard Walz IMAGING-PAM, found in many departments around the world, into a medium throughput phenotyping platform. We have designed a Python and R-based open source toolkit that allows for semi-automated sample segmentation and data analysis thereby reducing the processing bottleneck of large experimental datasets. We provide detailed instructions on how to build and functionally test each setup.

Conclusions: With material costs well below $1000, it is possible to setup a fluctuating light rack including a constant light control shelf for comparison. This allows more scientists to perform experiments closer to natural light conditions and contribute to an emerging research field. A small addition to the IMAGING-PAM not only increases sample throughput but also enables larger-scale plant phenotyping with automated data analysis.

Keywords: photosynthesis, phenotyping, fluctuating light, data analysis automation, do-it-yourself, maker movement

Background

In nature, plants frequently experience rapidly changing light conditions. This phenomenon is mainly caused by shading effects within the plant canopy or between neighboring plants. Additionally, cloud movements and pollutants cause changes in the light quality and quantity (Slattery et al., 2018). Plants have evolved several molecular mechanisms for coping with light stress of which the most important one is non-photochemical quenching (NPQ) (Jahns and Holzwarth, 2012). NPQ protects the plant effectively during high light by dissipating light energy as heat rather than allowing the energy to be put towards photochemistry. However, plants rapidly deactivate NPQ to maximize productivity when light availability becomes limiting. A number of enzymes and transport proteins critical in this process have been discovered over the last years (Armbruster et al., 2017). This was mainly achieved by switching from constant to dynamic growth lights mimicking natural conditions. More researchers should employ dynamic growth regimes to address open questions, but professional chambers with controllable LED elements and tools to determine photosynthesis come at a high cost.

Pulse-Amplitude-Modulation (PAM) chlorophyll fluorescence measurements represent a centerpiece of fitness evaluation for plants, algae and cyanobacteria (Brooks and Niyogi, 2011). Although primarily aimed at providing quantitative insight into the photosynthetic light reactions, several parameters determined during the measurements were found to be reliable indicators of a plant's response towards abiotic and biotic stresses (Murchie and Lawson, 2013). Notably, chlorophyll fluorescence fluorometers are frequently used detectors in automated phenotyping platforms. However, automated phenotyping requires significant investment and therefore platform installations and usage remain limited to few institutions worldwide.

Since its release in the mid-2000s, the Walz IMAGING-PAM, a manual bench-top camera-based chlorophyll fluorometer, has been widely applied in various types of research on phototropic organisms around the world (Escher et al., 2006). A brief Google scholar inquiry using the search term "IMAGING-PAM" yielded over 2300 results. Even though the machine offers many useful features, sample throughput and downstream data analysis are slow and cumbersome. These limitations have made it difficult to apply the IMAGING-PAM in larger scale experiments which are needed to unveil more subtle performance differences with low statistical power and for screening mutant or germplasm collections under an ever-increasing variety of treatment conditions. Experiment complexity and size are further expanded when previously published mutants are included as reference points.

Downstream data processing can benefit greatly from making subtle hardware adjustments. Consistent sample positioning and image capture settings facilitate scriptable image analysis tools (Tovar et al., 2018). Since no standardized imaging setup exists for the IMAGING-PAM, we tackled the issue by designing an easy-to-build sample holder kit which enables easy plant handling and guarantees consistent and reproducible positioning of individuals between experiments. Together these changes improve picture quality, increase sample throughput, and enable a more automated downstream data analysis pipeline.

Results

Order parts to build a low-cost plant growth rack for dynamic light experiments

Initially, all parts were purchased online. Table 1 summarizes each manufacturer and the item numbers. The items and pricing represent a loose guideline and might be outdated at the time of reading this article. Parts by other manufacturers may work just as well and may provide even cheaper options. However, the parts listed were thoroughly tested in this study and all parts work well together.

Setup of a low-cost plant growth rack for dynamic light experiments

Initially, the wire shelving rack was assembled with three levels according to the manufacturer's instructions. The distance between the shelves' lowest to highest point was 39 cm (Figure 1A). Hanging from the middle shelf, the shop LEDs for the constant light section were fixated using simple zip ties. It is important to use shop LEDs that can be daisy chained as this simplifies the control of the entire rack. The two light fixtures were hung on the most outside position and had a distance of 29.5 cm to each other (Figure 1B). Light intensities on the Arabidopsis leaf rosette level were found to be consistent around 90 µmol photons m^{-2} s^{-1}. The capacity of our constant light setup is 200 2" square pots.

Another pair of shop LEDs was installed similarly one shelf above to function as the background light for a dynamic light system. Both LED shop light units were individually plugged into a surge-protected power strip with integrated timer function set to 12 h on from 8 AM to 8 PM. Between the upper background lights, two 1500 W LED panels were positioned and strapped onto the rack using zip ties (Figure 1B-C). The distance between the two panels was 21 cm. These two 1500 W LED units were also cable-connected with each other. The single cable from the 1500 W LED panel unit was plugged into one of the "normally off" outlet in the controllable Outlet Power Relay Module (Figure 1D). Light intensities on the Arabidopsis leaf rosette level were on average 900 µmol photons m^{-2} s^{-1} when both the background LEDs and the two 1500 W LED panels run simultaneously. The entire installation should be inspected by a certified electrician to ensure the unit complies with local safety standards. The capacity of our fluctuation light setup is 90 2" square pots. This number is reduced from the lower shelf because the 1500W LED units provide a smaller band of illumination compared to the shop lights.

A rigid, dark, and opaque hard plastic cover was cut and put on the middle shelf to protect plants on the lower shelf from the high light intensities above. The plastic cover also prevents water spill into the electric equipment below. Lastly, the posts were cut off right above the shelf holding the two 1500 W LED panels. All new ends should be filed down and capped with standard 1" inner diameter plastic caps to avoid injuries. Because the 1500 W LED panels produce heat and have fan openings, it is not safe to use the space directly above. This also guided our decision to install the fluctuating light system in the upper half of the shelving.

The remaining post pieces (~65 cm length) and the last wire shelf were later used to build a smaller, secondary growth rack by adding an additional set of shop LEDs and one additional 1500 W LED panel with an opaque divider in the middle of the shelf (Additional file 1A). We used the same Outlet Power Relay Module so we were able to increase our capacity (27 additional plants under fluctuating light and 50 additional plants under constant light) for only ~$210.00.

121 A simple Adafruit micro-controller was connected to the Outlet Power Relay Module to
122 control the light pulses (i.e. output from the 1500 W LED panels). It was flashed with a script
123 (Additional file 2) that turns on the "normally off" outlet every 5 minutes for exactly one minute
124 (Figure 1D). Therefore, the plants become exposed to alternating high light (1 min at 900 µmol
125 photons m^{-2} s^{-1}) and low light (4 min at 90 µmol photons m^{-2} s^{-1}) (Additional file 1B). Minor
126 adjustments to the script could enable other light pulse frequencies or durations. The micro-
127 controller itself receives its power via the "always on" outlet on the Power Relay Module. The
128 Power Relay Module was connected to the timer-controlled power strip (12 h on from 8 AM to 8
129 PM). To protect the micro-controller unit from moisture it is strongly advisable to use a
130 weatherproof enclosure.

131 *Testing of the dynamic light plant growth rack using known loss-of-function mutants*

132 Among the best described Arabidopsis mutants susceptible to dynamic light are *stn7* and
133 the *pgr5* loss-of-function mutants. While *stn7* shows strongly diminished growth under fluctuating
134 light, *pgr5* is even more sensitive to the same conditions and dies rapidly after being shifted into
135 dynamic light (Tikkanen et al., 2010). Therefore, both loss-of-function lines serve as ideal controls
136 to test how closely the newly constructed growth rack reproduces previously published results
137 from independent international research groups.

138 STN7 represents a thylakoid serine-threonine protein kinase that phosphorylates Light
139 Harvesting Complex (LHC) II to allow for migration of the complex from photosystem II (PSII)
140 to PSI. The lack of this kinase therefore renders *stn7* loss-of-function mutant unable to adapt to
141 changing light conditions adequately (Bellafiore et al., 2005; Bonardi et al., 2005). Firstly, *stn7*
142 and WT were germinated and grown in 12/12 h day-night cycles using constant lighting (90 µmol
143 photons m^{-2} s^{-1}) on the lower shelf. At an age of 14 days, half the plants from each genotype
144 remained on the lowest shelf whereas the other half was moved onto the upper shelf where plants
145 were exposed to the previously described dynamic light conditions (1 min at 900 µmol photons
146 m^{-2} s^{-1}, 4 min at 90 µmol photons m^{-2} s^{-1}; 12/12 h day-night cycles at ambient room temperature).
147 At a plant age of four weeks, size differences between the two light treatments became clearly
148 visible. There was no growth difference between the genotypes under constant light, but *stn7*
149 revealed visually less leaf surface than WT under dynamic light (Figure 2A). Both observations
150 are in line with previously reported characteristics of *stn7* (Tikkanen et al., 2010; Grieco et al.,
151 2012). Additionally, when photosynthesis-related parameters of dark-adapted plants were
152 determined, *stn7* revealed reduced F_v/F_m values (Maximum quantum yield of PSII (Maxwell and
153 Johnson, 2000)) indicative of increased photoinhibition, i.e. PSII damage, under long-term
154 fluctuating light treatments (Figure 2B).

155 The extreme sensitivity of *pgr5* loss-of-function mutants to dynamic light has been
156 reported many times by independent groups (Suorsa et al., 2012; Thormählen et al., 2017; Trinh
157 et al., 2019). The susceptibility is primarily attributed to a malfunctioning cyclic electron flow
158 (CEF) cycle around PSI (Munekage et al., 2002). Therefore, *pgr5* was also tested in our newly
159 developed low-cost growth setup. Because of the sensitivity to fluctuating light, *pgr5* and a set of
160 WT plants were initially grown under constant light (12/ 12 h day-night cycles) for two weeks and
161 then shifted from the lower shelf into the dynamic light on the upper shelf. No *pgr5* mutant

individuals survived fluctuating light treatment longer than five days while all control plants performed well (Figure 2C).

In summary, the data obtained show that our cost-effective fluctuating light plant growth rack delivers comparable results to previously published studies that used higher cost commercial solutions. The rack is easy to setup and, with costs below $650, represents a useful alternative for research groups with limited financial resources.

Design of a sample holder kit for the IMAGING-PAM to improve throughput and data quality

The IMAGING-PAM can produce excellent images of chlorophyll fluorescence, but we found a few small additions to greatly improve the user experience by streamlining downstream analysis. The cost-effective plant growth racks described above enable more biological repetitions that include wild-type controls grown under both constant light and fluctuating light. To keep up with processing increasingly larger datasets, we reconfigured our IMAGING-PAM device to produce images with consistent plant placement and lighting conditions to facilitate more automation in the downstream analysis.

The sample holder kit includes a sample crate and standardized pot holder. First, a sample crate was built to accommodate nine 2” x 2” x 2⅛” pots ideal for growing single Arabidopsis plants (Figure 3A). The inner height of the crate was determined to ensure perfect camera focus at the lowest magnification. Second, holders for nine 2” square pots (Figure 3B, Additional file 3) were milled using PVC (an alternative option is also for four 3” square pots (Additional file 3)). A small notch was added to the upper right corner of the holders to allow for easy handling and consistent positioning of the plant holders even in the darkness when assaying dark-adapted plants. The height of the holders can be adjusted using the screws on each corner and should be fixed with a nut to fit the pots in the exact same vertical and horizontal position. All parts were made from standard PVC hard plastic, but other materials may be cheaper and perform equally well. However, it important to use opaque, low reflectance materials. All detailed technical schematics can be found in Additional file 3. Scientists working at institutions without machine shop are welcome to contact the corresponding author for assistance ordering through the Instrument Shop at WSU.

Although the working distance between the plants in the nine-plant pot holder and the camera lens is 2.6 cm longer than the 18.5 cm recommended by the manufacturer, this has no detectable effect of the image quality and the light pulse intensity. As shown in Figure 4, the reconfigured IMAGING-PAM delivers perfect plant images (F_v/F_m, NPQ shown in false colors) using *A. thaliana* wild-type plants vs. previously published *npq4-1* (Li et al., 2000) and *npq2-1* mutants (Niyogi et al., 1998) (21 days old, 12/12, constant light), with constitutive low NPQ and constitutively increased NPQ, respectively. Furthermore, the consistency of the setup, i.e. static position of the plants, is conducive for smooth time-lapse movies. This aids in visually tracking growth rates or phenotypic changes dependent on the plant developmental stage in specific mutant individuals. The holders ensure that each individual pot, and with that each individual plant, are recorded in the same position every time. The result is a much smoother time-lapse movie without the effect of plants bouncing around because of the difficulty of repositioning the plants in the same place for every measurement.

Efficient analysis of images recorded with an IMAGING-PAM

The ImagingWinGigE freeware by Walz is highly useful to control the IMAGING-PAM. Additionally, its script function provides an option to run customized measurement protocols. However, the downstream analysis is cumbersome and time-consuming because each pim file (its native format) must be loaded separately and areas-of-interest (AOI, or region-of-interest ROI as it is commonly called) need to be manually assigned. The development of the sample crate and plant pot holder to fix the plant positions (Figure 3A-B) was largely motivated by the desire to automate the analysis of multiple files. Automation requires that sample plants always appear in the same location of an image, which our efforts described above accomplish as long as the camera settings are not changed.

We developed an ImagingPAMProcessing toolkit that includes scripts in Python and R to automate the phenotype extraction from a stack of measurement files and visualize the results. These scripts can be downloaded as a .zip via GitHub (https://github.com/CougPhenomics/ImagingPAMProcessing). The scripts in their current version feature: 1) automated plant recognition (leaf segmentation) in Python using PlantCV (Gehan et al., 2017). 2) automated genotype assignment from a separately provided metadata file 3) calculation of F_v/F_m, NPQ, YII (the Quantum yield of PSII), and plant surface area 4) false-color pictures to visualize heterogeneity 5) Rmarkdown report to visualize data quality and trends in the phenotypes 6) R script to create time-lapse videos of false-color pictures of each of the photosynthetic parameters.

ImagingPAMProcessing Toolkit Setup

There are three main files that comprise the toolkit. The main script that processes the images is ProcesssImages.py while postprocessingQC.Rmd and makeVideos.R facilitate visualizations. There are a few prerequisite steps before using the ImagingPAMProcessing toolkit:

1. The PIM files must be exported to a generic format, i.e. TIFF, which can be accomplished with the ImagingWinGigE software either manually (Figure 5) or by adding the "Export to Tiff File=" command at the end of running a custom ImagingWinGigE script. See diy_data/LemnaTec2.prg for an example. This results in a multi-frame TIFF file with the same structure as the PIM file.

   The filenames of the multi-frame TIFF files must be standardized with hyphens to uniquely identify each measurement protocol. For instance, in the example dataset: treatment (control or fluc), the date of measurement (formatted YYYYMMDD), and the sample id (tray #) to identify the files: fluc-20190901-tray2.tif
2. We use two configuration files, or metadata maps, to provide more information for downstream analysis. First, pimframes_map.csv contains the definition of each frame of the TIFF file and the corresponding induction period. The order of the frames is standardized from Walz and the first four frames will not change between protocols. The frames of the TIFF files are arranged such that frames one and two are Fo and Fm, respectively, and frames three and four Red Absorptivity and NIR Absorptivity, respectively. Additional frames come in pairs (five/six, seven/eight, etc) where each pair correspond to F'/Fm' fluorescence measurements in the order they were captured. Note, if

Fo and Fm were measured as the initial induction period, then these frames are repeated in frames five/six. There are 34 frames resulting from the default induction curve protocol accessed through the ImagingWin Induction Curve tab. Correspondingly, our pimframes_map.csv includes entries for frames 1-34, with 15 different induction periods (F_v/F_m and 14 additional pairs of *F'/Fm'*). The second configuration file is called genotype_map.csv and relates the genotype to the tray number and ROI position. An example of both files is provided in the GitHub repository.

ProcessImages.py Customizations

In addition to the two configuration files, the user must update the `indir` variable in ProcessImages.py to point to their data directory. Additionally, there are three pieces of the image processing that may need to be adapted to the specific users' imaging setup:

1. Image segmentation is generally quite specific to the imaging conditions. An automated estimate for the initial threshold value is provided based on Yen's Algorithm (Yen et al., 1995), which is an entropy-based method implemented in the Python package scikit-image (van der Walt et al., 2014). This is followed by cleaning steps to remove small noise in the mask. In particular, we expect the cleaning steps found in src/segmentation/createmasks.py may need to be modified to adapt to unique imaging conditions from individual IMAGING-PAM setups. It should be noted that severe algae and moss growth due to overwatering will contaminate the images and make the image segmentation difficult. For more guidance on image segmentation we refer the reader to the excellent tutorials hosted by PlantCV (https://plantcv.readthedocs.io).
2. It is also likely the user will need to modify the locations of the ROIs to indicate where the plants are in the image. Even if using the 9 plant arrangement with the sample crate and 9 plant pot holders described in the text, it is likely the camera working distance will be slightly different and therefore the plant positions will be different relative to the image frame. In this case the location of the ROIs must be changed in the call to `pcv.roi.multi()` in scripts/ProcessImages.py. ROI coordinates can be adapted and visualized by stepping through the analysis with a single image with `pcv.params.debug = "plot"`. See the PlantCV documentation for details.
3. Our script outputs plant area that is automatically determined from the object detection algorithm implemented through PlantCV. It is important that each user updates the `pixel_resolution` variable for their own IMAGING-PAM setup to accurately convert pixels to mm^2. This variable will be specific to the camera and working distance and can be found near the top of the main python script. This needs only be performed once as long as the camera settings remain constant. We recommend imaging a plant with a hole punch of a known size and then measuring the width in pixels of the hole using ImageJ. `pixel_resolution` is then calculated as diameter in mm of hole punch divided by diameter in pixels of hole punch.

Post-Processing Report

In addition to the main python script for processing the image files, we also developed a report using RMarkdown (the source is found in the GitHub repository under

284 reports/postprocessingQC.rmd) that can be compiled to html (Additional file 4) and is intended to
285 provide a story-board-like overview of the extracted phenotypes. The user adjusts the variable
286 `datadir` to point to the directory which contains the input images. Our first analysis shows
287 whether all the data is present and if any of the QC flags were activated during image processing.
288 In particular, we are interested in whether each plant was completely imaged and whether the
289 plants remained independent in the image, i.e. did not overlap with each other at a given time point.
290 A False value for each of these tests invalidates the results of the image processing and motivate
291 the removal of these data points from further analysis. The next focus of the post-processing report
292 is to visualize the trends in each phenotype for each plant. We plot timeseries of plant area, YII,
293 and NPQ with bar plots and line plots because each plot type has unique advantages. Plotting using
294 a prescribed pipeline makes it trivial to generate an array of figures quickly and simultaneously.
295 Bulk visualization becomes important with more data being collected because it gives the
296 researcher a starting point to identify the most interesting features of the data. It is also easy to
297 identify data points that are out of range compared to the rest of a mutant panel. We find the
298 RMarkdown report advantageous compared to separate plots because each section can be
299 annotated and reads like a picture book story. For example, in section 7 of our report, we are
300 interested in the treatment effects. We clearly labeled the question we are interested in, can refer
301 to the data manipulation used, and can evaluate multiple figures to address the questions. At the
302 end we can compile any set of figures as required for publications (e.g. Figure 6).

303 *Time-lapse Movies*

304 Lastly, it is noteworthy that the ImagingPAMProcessing toolkit contains
305 scripts/makeVideos.R which can compile F_v/F_m, YII, NPQ false color time-lapse movies into
306 small-sized gifs which can be readily incorporated into slide presentations. The script
307 automatically annotates plants with their genotype and creates a movie for each pair of trays. As
308 mentioned earlier, the newly designed plant pot holders ensure that each individual plant is
309 recorded in the same position every time. The resulting time-lapse movies of the sample dataset
310 provided here can be found as Additional file 5.

311 *Testing the ImagingPAMProcessing toolkit using a diverse mutant panel recorded with the*
312 *IMAGING-PAM*

313 We employed the newly built growth rack (Figure 1) to record an eleven-day timeline of
314 Arabidopsis loss-of-function mutants grown under two different light treatments to showcase the
315 power and versatility of the ImagingPAMProcessing scripts. Specifically, we chose the *kea3*
316 mutant which is affected in K^+/H^+ exchange across the chloroplast thylakoid membrane
317 (Armbruster et al., 2014; Kunz et al., 2014) and the *vccn1/ best1* mutant affected in thylakoid Cl^-
318 ion flux (Duan et al., 2016; Herdean et al., 2016). Lastly, we added the previously mentioned *stn7*
319 mutant which is compromised in its capability to adapt to changing light conditions (Figure 2A-
320 B) (Bellafiore et al., 2005; Bonardi et al., 2005). The ion transport mutants served as points of
321 reference as they were recently characterized in a five day dynamic environmental photosynthesis
322 imager (DEPI) experiment (Cruz et al., 2016; Höhner et al., 2019). One half of the mutant panel
323 was kept on the lower shelf of the plant growth rack, i.e. exposed to constant light (90 µmol
324 photons m^{-2} s^{-1}, 12/12 h day-night cycle) throughout its three and half week life cycle. At an age
325 of 14 days, the other half of plants was exposed to fluctuating light on the upper shelf (1 min at

326 900 µmol photons m^{-2} s^{-1}, 4 min at 90 µmol photons m^{-2} s^{-1}; 12/ 12 h day-night cycles). Data
327 were recorded daily with the IMAGING-PAM for 11 days and plants photographed in true-color
328 at the end of this period (Figure 6A). A single day of phenotyping alone yielded 1,448 data points
329 (6 trays x 8 plants x 15 induction periods x 2 photosynthetic phenotypes + 48 estimates of plant
330 area). The 11-day screening period resulted in 16,368 data points, and more phenotypes might be
331 of interest in future experiments. Image standardization and a repeatable processing pipeline were
332 critical to analyze and inspect results in a time-effective manner.

333 We used the ImagingPAMProcessing toolkit to estimate and visualize plant size and
334 fitness. In doing so, it became obvious that the fluctuating light treatment adds a detrimental abiotic
335 stress to all genotypes (Figure 6B-D). WT and all mutants lost about half of their biomass
336 according to the surface area calculation our script performs. In general, WT plants always seemed
337 to grow best. However, because our proof-of-concept dataset had only four plant individuals per
338 genotype and per light treatment, we remain cautious to interpret any potential growth performance
339 differences among genotypes within either treatment group.

340 Photosynthetic fitness was evaluated with F_v/F_m and steady-state YII and NPQ. The F_v/F_m
341 plots revealed that only fluctuating light triggered genotype-specific F_v/F_m changes over time.
342 Initially, the onset of high light pulses damaged all genotypes (indicated by decreased F_v/F_m) for
343 the first 4 days (Figure 6E). WT and *kea3* eventually recovered PSII function and from thereon
344 revealed values slightly below non-treated control. However, loss of *KEA3* seemed to have a
345 protective effect on PSII, i.e. while the initial loss of F_v/F_m on the first day in fluctuating light was
346 equally strong as in WT, the recovery was faster such that *kea3* mutants reached equally high
347 F_v/F_m values but two days earlier than WT controls (Figure 6E-G). F_v/F_m in *vccn1* loss-of-function
348 mutants remained slightly below WT level, and *stn7* was clearly the most compromised mutant in
349 our panel with continuously progressing PSII damage in the presence of fluctuating light
350 throughout the experiment (Figure 6E-G).

351 In line with the documented damage to PSII (low F_v/F_m), steady-state YII also vanished
352 dramatically in *stn7* treated with fluctuating light (Figure 6H-J). Under the same light treatment,
353 the two ion transport mutants *kea3* and *vccn1* revealed only slightly diminished YII compared to
354 WT controls (Figure 6H, J).

355 We investigated steady-state NPQ among mutants in response to light treatments (Figure
356 6K-M). Under constant light, only *kea3* showed slightly elevated NPQ compared to WT (Figure
357 6K, M). This matches earlier results at similar light intensities (Armbruster et al., 2016). NPQ for
358 *stn7* mutants showed slightly depressed NPQ compared to WT whereas steady-state NPQ in *vccn1*
359 mostly behaved like the wild-type control (Figure 6K, M), confirming recent results (Duan et al.,
360 2016; Herdean et al., 2016). However, this situation changed when plants were treated with
361 fluctuating light. The effect on steady-state NPQ in *kea3* and *stn7* mutant lines became strongly
362 aggravated by fluctuating light in contrast to WT and *vccn1* (Figure 6K, L). In line with previous
363 reports (Armbruster et al., 2016; Höhner et al., 2019), NPQ was noticeably increased in *kea3*
364 compared to WT under the same conditions (Figure 6K, M) and compared to *kea3* plant mutants
365 grown under constant light (Figure 6K, L). The opposite effect was seen in the *stn7* mutant. In the

presence of high light pulses, NPQ decreased compared to WT under the same conditions (Figure 6K, M) and compared to *stn7* plant mutants grown under constant light (Figure 6K, L).

Discussion

Over the last decade, plant science and photosynthesis research has made a big push towards gaining insights into complex physiological, biochemical, and genetic processes under more realistic growth conditions than the traditional lab regimes in which growth environments are kept as constant as possible (Vialet-Chabrand et al., 2017; Andersson et al., 2019). In this respect, light regimes represent a good example because in nature light intensities are changing frequently (Slattery et al., 2018). So far, we have only scratched the surface of understanding the traits responsible for the rapid cellular acclimation to these irregular challenges. Therefore, it is important to empower more scientists globally with cost-effective tools so everyone can apply more natural but reproducible growth conditions. The work presented herein shows that employing fluctuating light conditions in plant science does not required high-priced commercially built LED setups housed in climate chambers. As long as a dark space at constant room temperature is available, a simple setup made from online ordered parts delivers congruent results. By providing detailed instructions and the script to control the LED panels (according to the most commonly published fluctuating light conditions published) everyone interested should be able to quickly assemble the parts to apply the same experimental light conditions (Figure 1).

Using previously published mutants *stn7* and *pgr5* (Figure 2), we successfully validated our experimental setup by achieving similar results compared to past work (Grieco et al., 2012; Thormählen et al., 2017). As new fluctuating light susceptible mutants are isolated, it is important to compare them with both WT and mutants with known phenotypes under constant and dynamic light in order to put the treatment effects in perspective. Our results provide confidence that experiments with our new plant growth racks will yield interesting and accurate phenotypes. A potential improvement to our design is to provide stronger background illumination as the 90 µmol photons m^{-2} s^{-1} is at the low end of the ideal *A. thaliana* light intensity range. Further, it would be advantageous to provide constant illumination closer to the average equivalent photon flux in the dynamic light conditions which is 252 µmol photons m^{-2} s^{-1}. The plant-to-light distance could be decreased to increase the photon flux in the constant light shelf at the expense of increased temperatures at the leaf level. Future experiments should evaluate the impact of this change.

Expanding experimental conditions and involving suitable, published genetic controls as a point of reference is good practice and highly advisable in light experiments. However, this also significantly expands the size of the experimental dataset and increases data analysis requirements. Employing automated phenotyping platforms with capabilities to record photosynthetic performance would be ideal but the high equipment costs can prevent access to phenotyping tools at most academic institutions. To cope with these challenges, we turned the most widely distributed camera-based chlorophyll fluorometer, the Walz IMAGING-PAM, into a semi-automated phenotyper with a few simple adjustments. A sample crate in combination with potholders (Figure 3) ensures that plants can be measured in the same spot even if moving the specimens in and out of the growth chamber is required. The slightly increased sample distance to the camera lens did not result in unfocused images or a detectable loss in measuring light intestines (Figure 4). All

407 schematics can be found online to replicate our system or parts can be ordered through us
408 (Additional file 3).

409 The minor positioning updates allowed us to design the ImagingPAMProcessing toolkit, a
410 new open source analysis pipeline specifically designed for increasing the throughput of the Walz
411 IMAGING-PAM. Scientists can now rapidly analyze and plot large and complex experimental
412 datasets from a fluorometer. The image processing scripts automatically attempts plant
413 segmentation to distinguish between leaf and background using the open source PlantCV
414 phenotyping toolbox (Gehan et al., 2017). Common photosynthetic phenotypes and plant area are
415 extracted per plant and can be visualized and analyzed in relation to treatment, time, and genotype.
416 We specifically focus on highlighting differences between a genotype control and a treatment
417 control and provide the ability to create time-lapse movies of each phenotype for each plant.

418 To validate the script and to provide interested users with a training dataset, we recorded
419 an eleven-day fluctuating light experiment using mostly genotypes recently tested in a five day
420 long Dynamic Environmental Photosynthetic Imaging run (Höhner et al., 2019) (Figure 6). In line
421 with earlier studies, we found that all genotypes were affected by dynamic light (Vialet-Chabrand
422 et al., 2017; Schneider et al., 2019). Leaf surface in WT plants decreased by more than half. As
423 reported before, we also saw evidence that growth of *stn7* mutants was especially impacted by
424 fluctuating light which triggered dramatic decreases in F_v/F_m and YII (Tikkanen et al., 2010;
425 Grieco et al., 2012). Our observations of steady-state NPQ and YII in thylakoid ion transport
426 mutants *kea3* and *vccn1* are also in line with other recent reports of these loss-of-function mutants
427 (Dukic et al., 2019; Höhner et al., 2019).

428 Conclusions

429 Dynamic or fluctuating growth light conditions represent a cornerstone in understanding
430 acclimation processes in photoautotrophic organisms. We have shown that high priced LED
431 climate chambers and phenotyping equipment are not necessarily required to unveil the underlying
432 genes involved in light stress acclimation processes. The simple construction of our micro-
433 controller based LED light racks and minor modifications to the IMAGING PAM allow the
434 application of our newly developed ImagingPAMProcessing toolkit. The wealth of data collected
435 and analyzed in this way can provide new and highly useful insights. The tools introduced here
436 are not limited to plant science but will also help to streamline genetic screens and physiology
437 experiments in algae and cyanobacteria. For instance, the use of micro-multiwell plates in fixed
438 positions in the IMAGING-PAM should allow for straight-forward application of the
439 ImagingPAMProcessing toolkit. Accordingly, we encourage others to pick up the open source
440 toolkit and adapt and expand it with new features.

441 Methods

442 *Plant growth conditions*

443 Wild type (WT) *Arabidopsis thaliana* accession Columbia-0 (Col-0) and mutant seeds
444 were EtOH surface sterilized, stratified for days at 4°C, and grown on ½ Murashige & Skoog (MS)
445 1 % (w/v) phytoagar plates pH 5.8 for one week at 90 µmol photons m^{-2} s^{-1} constant illumination
446 in a 12h/ 12h day-night cycle at 22°C. At an age of seven days, seedlings designated for constant

447 light conditions were potted into 2” x 2” x 2⅛” pots (Item #: 1665 by Anderson Pots, Portland,
448 OR, USA) and grown under the same light condition until the end of their life cycle.

449 If individuals were designated for fluctuating light treatment, plants were initially grown
450 for two weeks in constant light (90 µmol photons m^{-2} s^{-1}) and then moved into fluctuating light (1
451 min at 900 µmol photons m^{-2} s^{-1} and 4 min at 90 µmol photons m^{-2} s^{-1}) for two weeks.

452 Light intensities were careful monitored using a MQ-200 Quantum Separate Sensor with
453 Handheld Meter and a data logger (Apogee Instruments, Inc. Logan, UT, USA).

454 *Plant mutant isolation and information*

455 The *vccn1-1* (SALK_103612) T-DNA insertion line (Herdean et al., 2016) was ordered
456 from the ABRC stock center. Homozygous individuals were isolated through PCR-based
457 genotyping using the WT primer combination: *VCCN1* 5’ UTR fwd (5’-
458 3’: catgtcatgtgaagtgaagtgaag)/ *VCCN1* rev (GCTGCAATGTAACGAAGAAGC) yielding a 1129
459 bps product and the KO primer combination *VCCN1* 5’ UTR fwd (5’-
460 3’: catgtcatgtgaagtgaagtgaag)/ Salk LBb1.3 (5’-3’: attttgccgatttcggaac) to produce a ~ 500 bps
461 product.

462 *Accession Numbers for this study*

463 Additionally, the following homozygous loss-of-function mutant lines were employed in
464 this study: *npq4-1* (Li et al., 2000), *npq2-1* aka *aba1-6* (CS3772, Niyogi et al., 1998), *kea3-1*
465 (Gabi_170G09; Armbruster et al., 2014), *stn7-1* (SALK_073254, (Bellafiore et al., 2005; Bonardi
466 et al., 2005)), *pgr5-1* (Munekage et al., 2001).

467 *Pulse-Amplitude-Modulation (PAM) fluorescence spectroscopy*

468 A MAXI version IMAGING-PAM (IMAG-K7 by Walz, Effeltrich, Germany) was
469 employed in all experiments were photosynthesis-related parameters were recorded. Before each
470 measurements, plants were positioned in the newly designed plant holders. Subsequently, plants
471 were dark-adapted for 15 minutes followed by recording of a standard induction curve at 186 µmol
472 photons m^{-2} s^{-1} actinic light. All data were analyzed with the new ProcessImages.py script and for
473 comparison also using the ImagingWinGigE freeware by Walz.

474 Declarations
475 Ethics approval and consent to participate

476 Not applicable

477 Consent for publication

478 Not applicable

479 Availability of data and materials
480 The scripts described in the text can be downloaded from
481 https://github.com/CougPhenomics/ImagingPAMProcessing and the accompanying 11 day
482 dataset can be downloaded from https://doi.org/10.17605/OSF.IO/P32AY

Competing interests

The authors declare that they have no competing interests.

Funding

HHK received funding from an NSF Career Award IOS-1553506 and the 3rd call ERA-CAPS call via the NSF PGRP program. Furthermore, support came from the DOE-BES program (#DE-SC0017160) to HK. The project was also made possible thanks to an equipment grant by the Murdock trust to HHK.

Authors' contributions

HHK designed the research and the sample holder kit, built the dynamic light growth racks, and wrote the manuscript. DS programed the PSII processing pipeline, coded the R data potting toolkit, analyzed experimental data, designed figures, wrote sections of the manuscript, and edited the manuscript. LSL carried out all plant experiments, analyzed experimental data, and designed figures. JDC wrote the micro-controller script. ML and HK isolated *vccn1-1* line and edited the manuscript. DMS designed and built the PAM crate and plant holders. All authors read and approved the final manuscript

Acknowledgements

We thank Dave Savage from the Technical Services Instrument shop at WSU for help with the design of sample kit. We are very grateful for advice on pim file conversion provided by the scientists at Walz. Furthermore, we thank Dr. Ute Armbruster at MPI Golm for providing *pgr5* mutant seeds. HHK thanks The Helen Riaboff Whiteley Center and the people at the UW Friday Harbor Labs for providing a writing refuge.

References

Andersson, B., Shen, C., Cantrell, M., Dandy, D.S.,Peers, G. (2019). The Fluctuating Cell-Specific Light Environment and its Effects on Cyanobacterial Physiology. Plant Physiol.**,** pp.00480.2019.

Armbruster, U., Correa Galvis, V., Kunz, H.-H.,Strand, D.D. (2017). The regulation of the chloroplast proton motive force plays a key role for photosynthesis in fluctuating light. Current Opinion in Plant Biology **37,** 56-62.

Armbruster, U., Leonelli, L., Correa Galvis, V., Strand, D., Quinn, E.H., Jonikas, M.C.,Niyogi, K.K. (2016). Regulation and Levels of the Thylakoid K^+/H^+ Antiporter KEA3 Shape the Dynamic Response of Photosynthesis in Fluctuating Light. Plant Cell Physiol. **57,** 1557-67.

Armbruster, U., Carrillo, L.R., Venema, K., Pavlovic, L., Schmidtmann, E., Kornfeld, A., Jahns, P., Berry, J.A., Kramer, D.M.,Jonikas, M.C. (2014). Ion antiport accelerates photosynthetic acclimation in fluctuating light environments. Nature communications **5,** 5439.

Bellafiore, S., Barneche, F., Peltier, G.,Rochaix, J.-D. (2005). State transitions and light adaptation require chloroplast thylakoid protein kinase STN7. Nature **433,** 892-5.

522 **Bonardi, V., Pesaresi, P., Becker, T., Schleiff, E., Wagner, R., Pfannschmidt, T., Jahns,**
523 **P.,Leister, D.** (2005). Photosystem II core phosphorylation and photosynthetic acclimation
524 require two different protein kinases. Nature **437,** 1179-82.
525 **Brooks, M.D.,Niyogi, K.K.** (2011). Use of a Pulse-Amplitude Modulated Chlorophyll
526 Fluorometer to Study the Efficiency of Photosynthesis in Arabidopsis Plants. In
527 Chloroplast Research in Arabidopsis: Methods and Protocols, Volume II, R.P. Jarvis, ed
528 (Totowa, NJ: Humana Press), pp. 299-310.
529 **Cruz, J.A., Savage, L.J., Zegarac, R., Hall, C.C., Satoh-Cruz, M., Davis, G.A., Kovac, W.K.,**
530 **Chen, J.,Kramer, D.M.** (2016). Dynamic Environmental Photosynthetic Imaging Reveals
531 Emergent Phenotypes. Cell Systems **2,** 365-77.
532 **Duan, Z., Kong, F., Zhang, L., Li, W., Zhang, J.,Peng, L.** (2016). A bestrophin-like protein
533 modulates the proton motive force across the thylakoid membrane in Arabidopsis. Journal
534 of Integrative Plant Biology **58,** 848-58.
535 **Dukic, E., Herdean, A., Cheregi, O., Sharma, A., Nziengui, H., Dmitruk, D., Solymosi, K.,**
536 **Pribil, M.,Spetea, C.** (2019). K^+ and Cl^- channels/transporters independently fine-tune
537 photosynthesis in plants. Scientific Reports **9,** 8639.
538 **Escher, B.I., Quayle, P., Muller, R., Schreiber, U.,Mueller, J.F.** (2006). Passive sampling of
539 herbicides combined with effect analysis in algae using a novel high-throughput
540 phytotoxicity assay (Maxi-Imaging-PAM). Journal of Environmental Monitoring **8,** 456-
541 64.
542 **Gehan, M.A., Fahlgren, N., Abbasi, A., Berry, J.C., Callen, S.T., Chavez, L., Doust, A.N.,**
543 **Feldman, M.J., Gilbert, K.B., Hodge, J.G., Hoyer, J.S., Lin, A., Liu, S., Lizárraga, C.,**
544 **Lorence, A., Miller, M., Platon, E., Tessman, M.,Sax, T.** (2017). PlantCV v2: Image
545 analysis software for high-throughput plant phenotyping. PeerJ **5,** e4088.
546 **Grieco, M., Tikkanen, M., Paakkarinen, V., Kangasjärvi, S.,Aro, E.-M.** (2012). Steady-State
547 Phosphorylation of Light-Harvesting Complex II Proteins Preserves Photosystem I under
548 Fluctuating White Light. Plant Physiol. **160,** 1896-910.
549 **Herdean, A., Teardo, E., Nilsson, A.K., Pfeil, B.E., Johansson, O.N., Ünnep, R., Nagy, G.,**
550 **Zsiros, O., Dana, S., Solymosi, K., Garab, G., Szabó, I., Spetea, C.,Lundin, B.** (2016).
551 A voltage-dependent chloride channel fine-tunes photosynthesis in plants. Nature
552 communications **7,** 11654.
553 **Höhner, R., Galvis, V.C., Strand, D.D., Völkner, C., Krämer, M., Messer, M., Dinc, F., Sjuts,**
554 **I., Bölter, B., Kramer, D.M., Armbruster, U.,Kunz, H.-H.** (2019). Photosynthesis in
555 Arabidopsis Is Unaffected by the Function of the Vacuolar K^+ Channel TPK3. Plant
556 Physiol. **180,** 1322-35.
557 **Jahns, P.,Holzwarth, A.R.** (2012). The role of the xanthophyll cycle and of lutein in
558 photoprotection of photosystem II. Biochimica et Biophysica Acta (BBA) - Bioenergetics
559 **1817,** 182-93.
560 **Kunz, H.H., Gierth, M., Herdean, A., Satoh-Cruz, M., Kramer, D.M., Spetea, C.,Schroeder,**
561 **J.I.** (2014). Plastidial transporters KEA1, -2, and -3 are essential for chloroplast
562 osmoregulation, integrity, and pH regulation in Arabidopsis. Proc Natl Acad Sci U S A.
563 **111,** 7480-5.
564 **Li, X.-P., Björkman, O., Shih, C., Grossman, A.R., Rosenquist, M., Jansson, S.,Niyogi, K.K.**
565 (2000). A pigment-binding protein essential for regulation of photosynthetic light
566 harvesting. Nature **403,** 391.

Maxwell, K.,Johnson, G. (2000). Chlorophyll fluorescence - a practical guide. J Exp Bot **51,** 659 - 68.

Munekage, Y., Hojo, M., Meurer, J., Endo, T., Tasaka, M.,Shikanai, T. (2002). *PGR5* Is Involved in Cyclic Electron Flow around Photosystem I and Is Essential for Photoprotection in *Arabidopsis*. Cell **110,** 361-71.

Murchie, E.H.,Lawson, T. (2013). Chlorophyll fluorescence analysis: a guide to good practice and understanding some new applications. J Exp Bot. **64,** 3983-98.

Niyogi, K.K., Grossman, A.R.,Björkman, O. (1998). Arabidopsis Mutants Define a Central Role for the Xanthophyll Cycle in the Regulation of Photosynthetic Energy Conversion. Plant Cell. **10,** 1121-34.

Schneider, T., Bolger, A., Zeier, J., Preiskowski, S., Benes, V., Trenkamp, S., Usadel, B., Farré, E.M.,Matsubara, S. (2019). Fluctuating Light Interacts with Time of Day and Leaf Development Stage to Reprogram Gene Expression. Plant Physiol. **179,** 1632-57.

Slattery, R.A., Walker, B.J., Weber, A.P.M.,Ort, D.R. (2018). The Impacts of Fluctuating Light on Crop Performance. Plant Physiol. **176,** 990-1003.

Suorsa, M., Järvi, S., Grieco, M., Nurmi, M., Pietrzykowska, M., Rantala, M., Kangasjärvi, S., Paakkarinen, V., Tikkanen, M., Jansson, S.,Aro, E.-M. (2012). PROTON GRADIENT REGULATION5 Is Essential for Proper Acclimation of *Arabidopsis* Photosystem I to Naturally and Artificially Fluctuating Light Conditions. Plant Cell. **24,** 2934-48.

Thormählen, I., Zupok, A., Rescher, J., Leger, J., Weissenberger, S., Groysman, J., Orwat, A., Chatel-Innocenti, G., Issakidis-Bourguet, E., Armbruster, U.,Geigenberger, P. (2017). Thioredoxins Play a Crucial Role in Dynamic Acclimation of Photosynthesis in Fluctuating Light. Molecular Plant **10,** 168-82.

Tikkanen, M., Grieco, M., Kangasjärvi, S.,Aro, E.-M. (2010). Thylakoid Protein Phosphorylation in Higher Plant Chloroplasts Optimizes Electron Transfer under Fluctuating Light. Plant Physiol. **152,** 723-35.

Tovar, J.C., Hoyer, J.S., Lin, A., Tielking, A., Callen, S.T., Elizabeth Castillo, S., Miller, M., Tessman, M., Fahlgren, N., Carrington, J.C., Nusinow, D.A.,Gehan, M.A. (2018). Raspberry Pi–powered imaging for plant phenotyping. Applications in Plant Sciences **6,** e1031.

Trinh, M.D.L., Sato, R.,Masuda, S. (2019). Genetic characterization of a *flap1* null mutation in Arabidopsis npq4 and pgr5 plants suggests that the regulatory role of FLAP1 involves the control of proton homeostasis in chloroplasts. Photosynth Res **139,** 413-24.

van der Walt, S., Schönberger, J.L., Nunez-Iglesias, J., Boulogne, F., Warner, J.D., Yager, N., Gouillart, E.,Yu, T. (2014). scikit-image: image processing in Python. PeerJ **2,** e453.

Vialet-Chabrand, S., Matthews, J.S.A., Simkin, A.J., Raines, C.A.,Lawson, T. (2017). Importance of Fluctuations in Light on Plant Photosynthetic Acclimation. Plant Physiol. **173,** 2163-79.

Yen, J.-C., Chang, F.-J.,Chang, S. (1995). A new criterion for automatic multilevel thresholding. IEEE Transactions on Image Processing **4,** 370-8.

Figures and Tables

Table 1: Parts needed for construction of fluctuating light plant growth rack

Item name	**Manufacturer**	**Approximate cost**	**Number (optional)**
4-Tier Wire Shelving Rack, 48" x 24" x 72" NSF (SKU TBFPB-0916)	Trinity International Industries (Carson, CA, USA)	$95.00 - $120.00	1
1500W Double Chips LED panel Model: GLB1500	HIGROW LED	$148.00	2 (3)
2 Pack LED Utility Shop Light, 4 FT, Linkable Integrated Fixture, 40W=260W, 5000K Daylight, 4100 LM, Frosted Lens (SKU SH_F-40W-6K-2PK)	Sunco Lighting (Simi Valley, CA, USA)	$59.99	2 (3)
Opaque PVC	Hardware store	~$10.00	1
Zip Ties	Hardware store	~$10.00	1 bag (~100 pc)
standard 1” inner diameter plastic caps	Hardware store	~$10.00	1 (4 pc)
Wall Surge Protector with 4 Timer-Controlled Outlets (P4GC)	APC	$16.07	1
Adafruit METRO 328 Fully Assembled - Arduino IDE compatible - ATmega328	Adafruit	$17.50	1
Weatherproof Enclosure With PG-7 Cable Glands	Adafruit	$9.95	1
IoT Power Relay, Controllable Four Outlet Power Relay Module version 2 - (Power Switch Tail Alternative) PRODUCT ID: 2935	Digital Loggers	$24.95	1
Premium Male/Male Jumper Wires - 20 x 3" (75mm) PRODUCT ID: 1956	Adafruit	$1.95	1
	Approx. total costs:	**$640.31 ($848.30)**	

Figure 1.

Design of low-cost fluctuating light plant rack. A) Front view of the growth rack (120 cm total height). Control section at the bottom and fluctuating light (FL) section above with a height of 39 cm each. B) In both sections two daisy-chained LED shop lights were placed 29.5 cm apart from each other. Additionally, in the FL section, two daisy-chained 1500W LED panels were installed 21 cm away from each other. An opaque hard-plastic cover divides the FL from the control section. C) Side-view of the rack. D) The 1500W LED panels are plugged into a controllable outlet power relay module controlled by a micro-controller, which determines when the panels turn on and off (1 min at 900 µmol photons m^{-2} s^{-1} and 4 min at 90 µmol photons m^{-2}

623 s^{-1}). The outlet power relay module and the LED shop lights run on timer-controlled outlets that
624 keep both units on for 12hrs.

625 Figure 2.

626 Arabidopsis WT and *stn7* phenotypes under constant light (control), and fluctuating light
627 (FL). A) Four week old plants which were exposed to constant light (90 µmol photons m^{-2} s^{-1}) or
628 FL (1 min at 900 µmol photons m^{-2} s^{-1} and 4 min at 90 µmol photons m^{-2} s^{-1}) for the last two
629 weeks. *stn7* plants under FL revealed decrease growth and F_v/F_m values compared to WT under
630 fluctuating light. B) Bar graph of mean F_v/F_m (± SE, n=5). Asterisks indicate a statistically
631 significant difference compared with WT (***P<0.0001, two-way ANOVA). C) Four-week-
632 old plants exposed to FL. *pgr5* did not survive the treatment for more than 5 days compared to WT
633 under fluctuating light.

634 Figure 3.

635 Reconfiguration of the Walz IMAGING-PAM. A) Drawing and image of the newly
636 designed sample crate. B) Sample crate inserted in the IMAGING-PAM. C) Drawing and image
637 of newly designed 9-pot-holders. Pot dimensions: 2" x 2" x 2⅛". The holders fit perfectly into the
638 sample crate. The height of the holders can be adjusted with screws to ensure ideal pot-holder fit.

639 Figure 4.

640 The reconfigured IMAGING-PAM with the newly designed sample crate and holders
641 delivers perfectly focused false color images and values (F_v/F_m and non-photochemical quenching
642 NPQ/4) of four week old *npq4-1*, wild-type, and *npq2-1* plants grown in constant light (90 µmol
643 photons m^{-2} s^{-1}).

644 Figure 5.

645 Schematic showing the critical steps to setup and run the scripts in the
646 ImagingPAMProcessing toolkit.

647 Figure 6.

648 Data analysis from 11 day long phenotyping experiment. A) Four week old mutant lines
649 and WT control plants after being subjected to constant or fluctuating light conditions. B-D)
650 Growth behavior, E-G) F_v/F_m, H-J) YII, and K-M) NPQ throughout the experiment.

651 Additional Files
652

653 Additional File 1.

654 A) Background and fluctuating light mode of the growth racks. B) Extension or single unit
655 fluctuating light shelf. Shown are both operation modes.

656 Additional File 2.

657 Fluctuating light script to flash the Adafruit (Arduino-type) micro-controller.

Additional File 3.

Schematics of the sample holder kit. Sample crate and plant pot holders are compatible with the IMAGING PAM.

Additional File 4.

Post-processing quality control output generated by the ImagingPAMProcessing toolkit. The proof-of-concept dataset from this was used for this output example.

Additional File 5.

Time-lapse movies for F_v/F_m, steady-state YII, and steady-state NPQ generated from the proof-of-concept dataset.

Figure 1

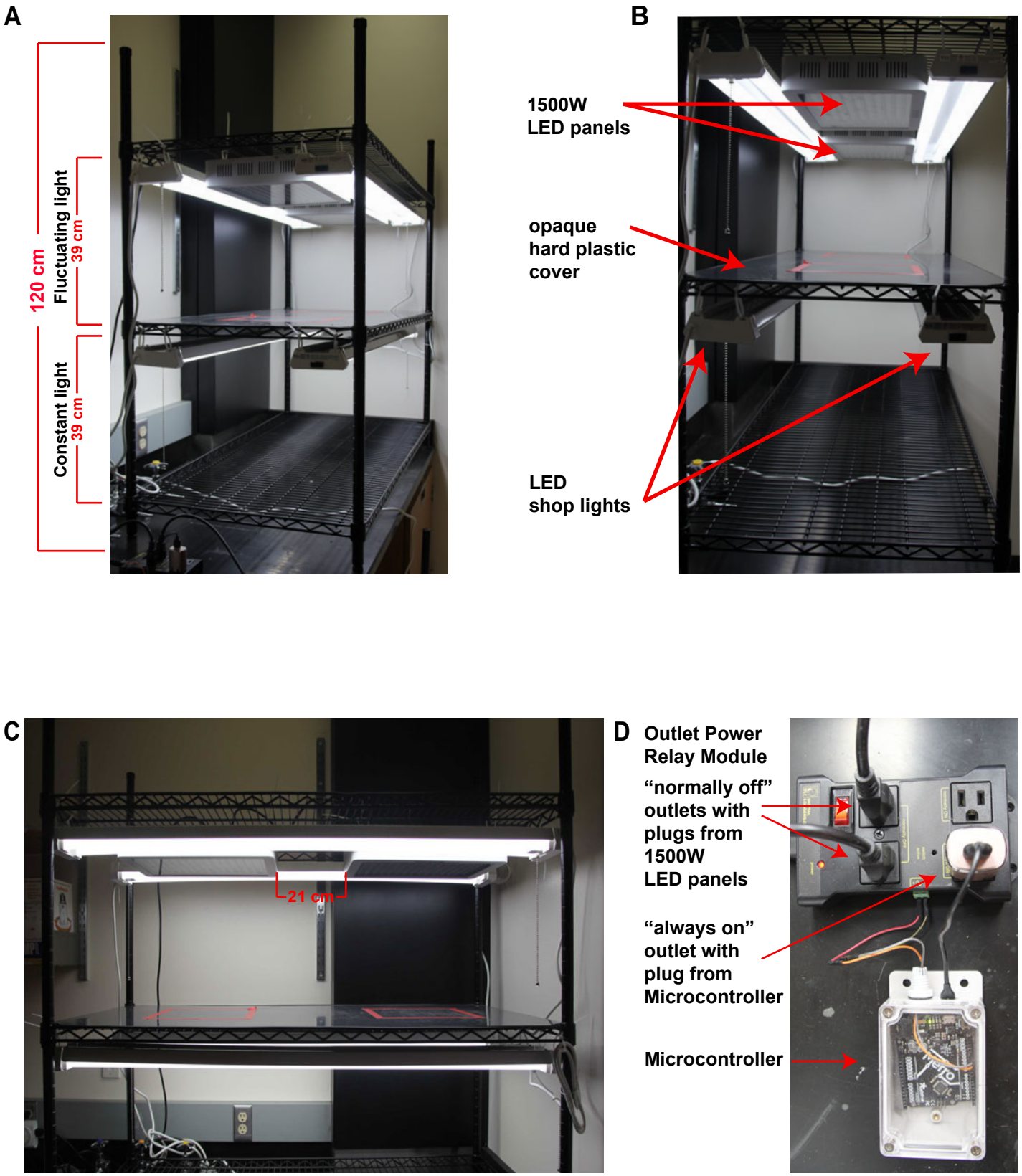
A
120 cm
Fluctuating light
39 cm
Constant light
39 cm
B
1500W
LED panels
opaque
hard plastic
cover
LED
shop lights
C
21 cm
D
Outlet Power
Relay Module
"normally off"
outlets with
plugs from
1500W
LED panels
"always on"
outlet with
plug from
Microcontroller
Microcontroller

Figure 2

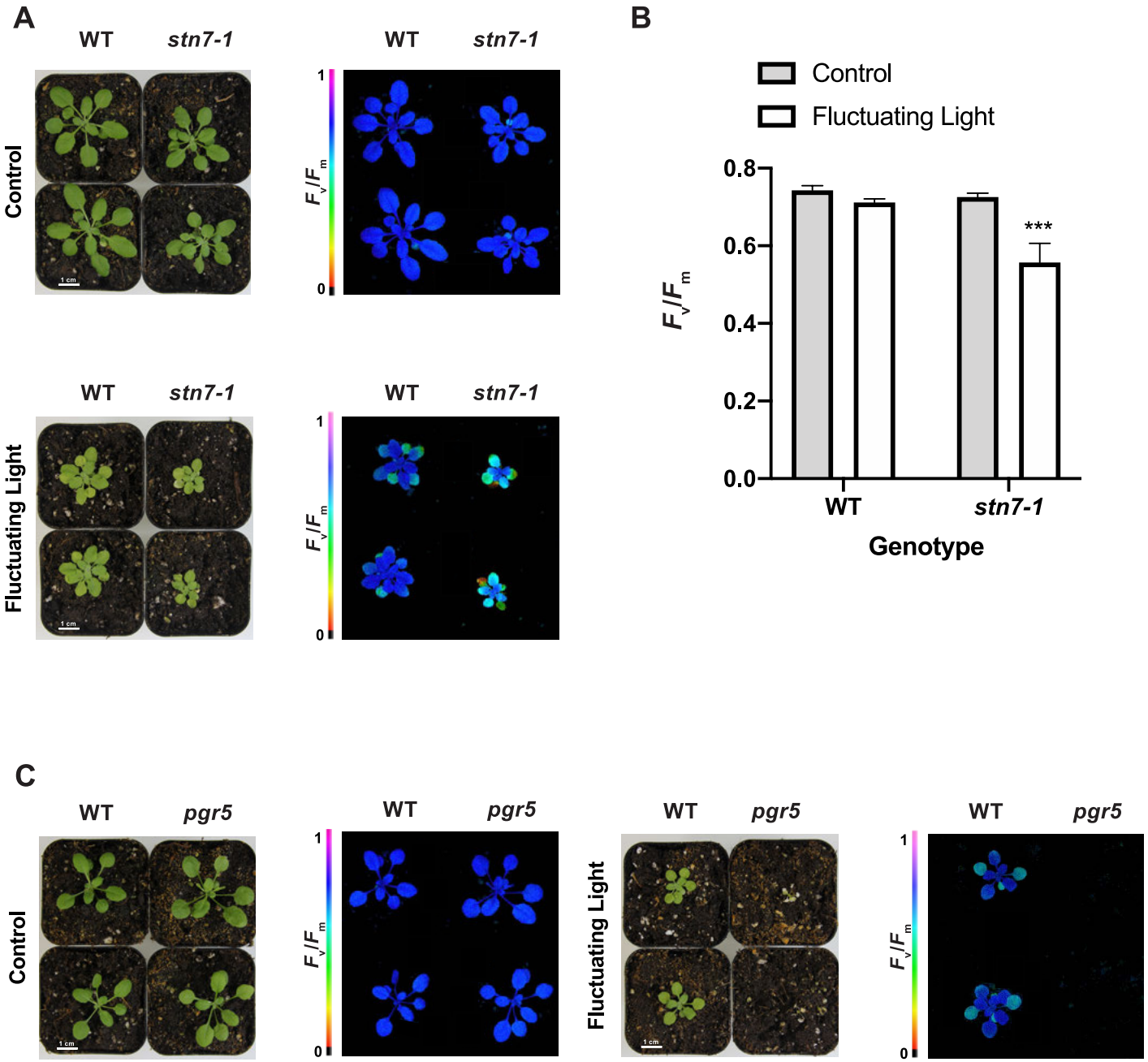
A
WT
stn7-1
Control
Fluctuating Light
1 cm
1
0
F_v/F_m
B
Control
Fluctuating Light
0.8
0.6
0.4
0.2
0.0
***
WT
stn7-1
Genotype
C
pgr5

Figure 3

A

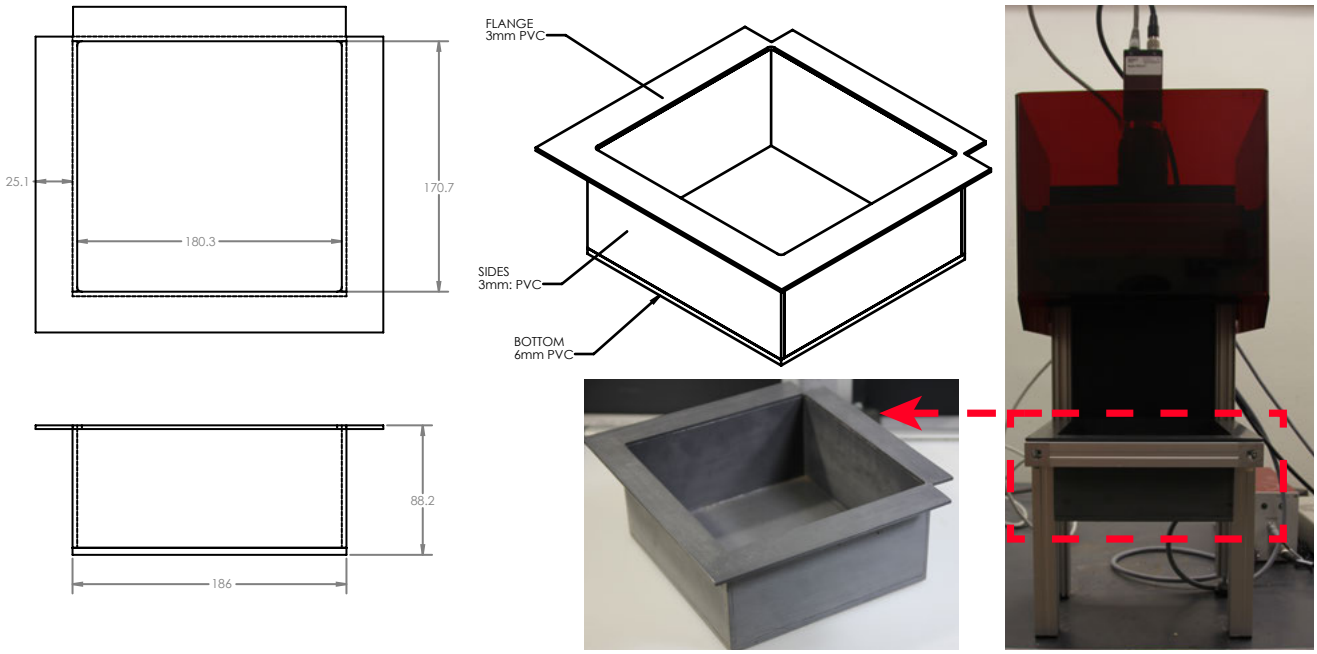
25.1
180.3
170.7
88.2
186
FLANGE
3mm PVC
SIDES
3mm: PVC
BOTTOM
6mm PVC

B

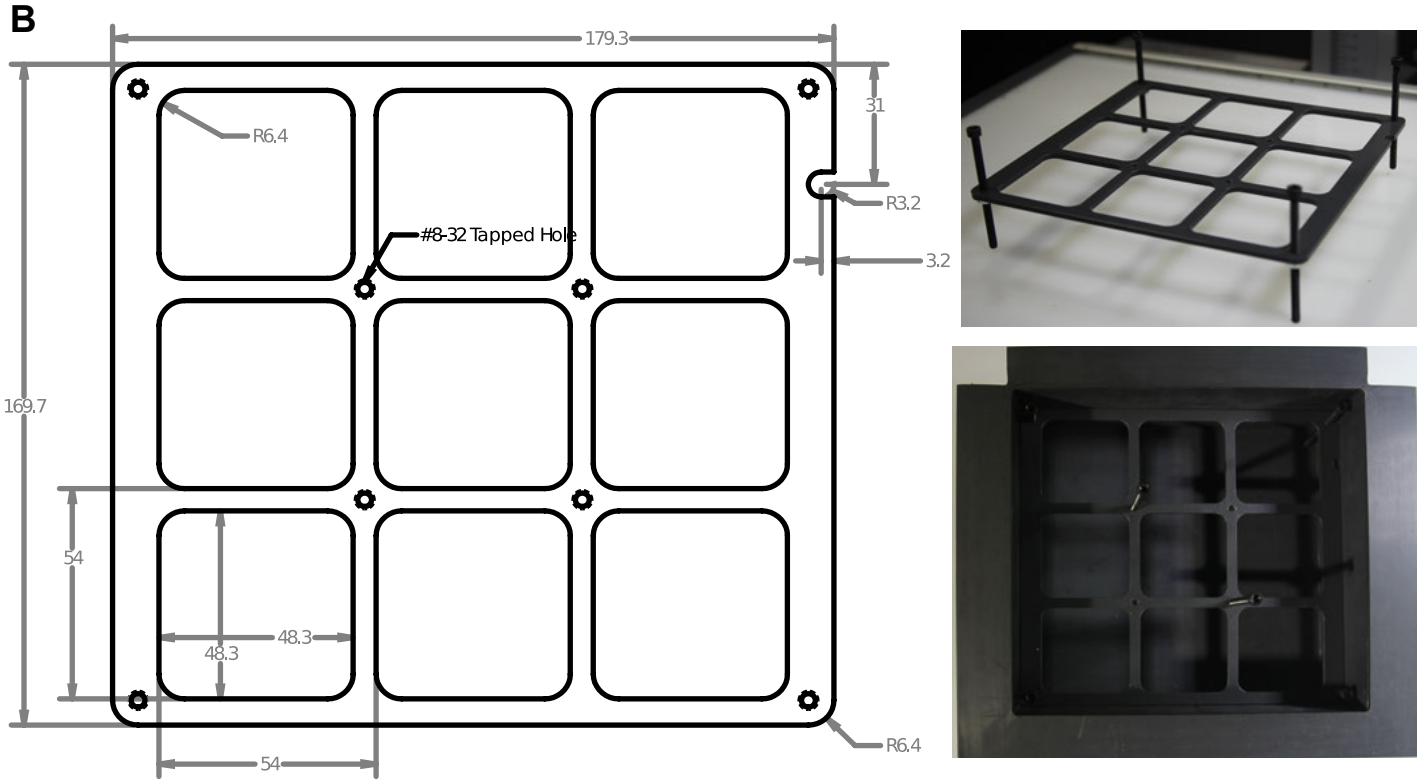
179.3
31
R6.4
R3.2
#8-32 Tapped Hole
3.2
169.7
54
48.3
48.3
54
R6.4

Figure 4

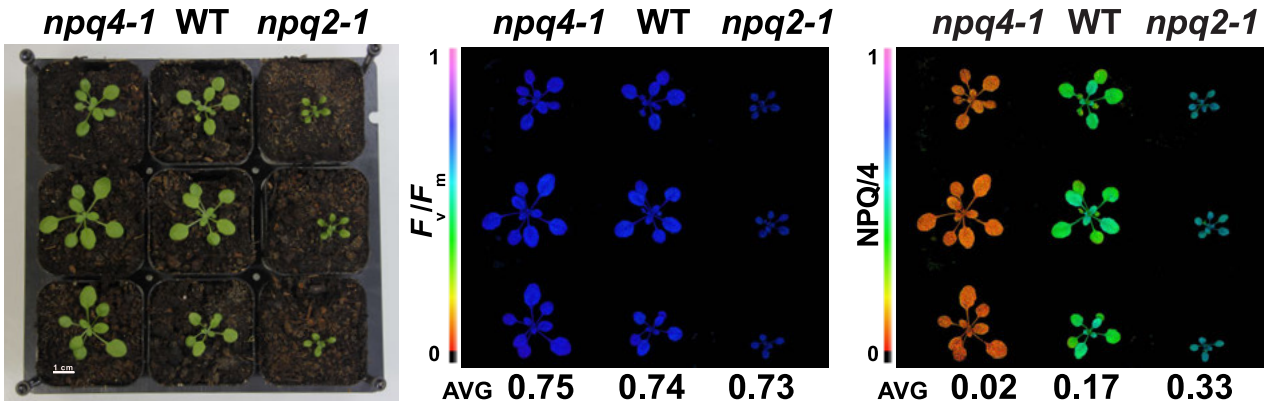
npq4-1 WT npq2-1
1 cm
npq4-1 WT npq2-1
1
0
F_v/F_m
AVG 0.75 0.74 0.73
npq4-1 WT npq2-1
1
0
NPQ/4
AVG 0.02 0.17 0.33

Figure 5

Setup

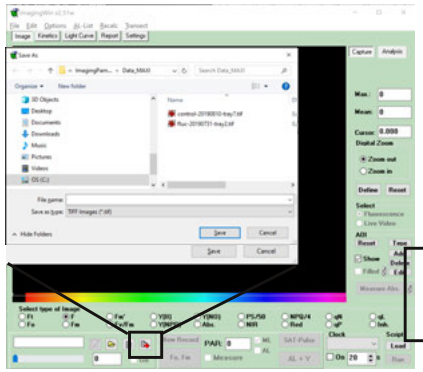

1. convert .pim files
2. name files correctly
3. metadata maps

diy_data > raw_multiframe

Name

- control-20190731-tray5.pim
- control-20190731-tray5.tif
- control-20190731-tray6.pim
- control-20190731-tray6.tif
- control-20190731-tray7.pim

diy_data > pimframes

Name

- control-20190731-tray6-15.tif
- control-20190731-tray6-16.tif
- control-20190731-tray6-10.tif
- control-20190731-tray6-11.tif
- control-20190731-tray6-12.tif

auto-created in ProcessImages.py

DIY > diy_data >

Name

- pimframes
- raw_multiframe
- genotype_map.csv
- LemnaTec2.prg
- pimframes_map.csv

diy_data > pimframes_map.csv

```
imageid,frame,param
1,Fo,FvFm
2,Fm,FvFm
3,AbsR,AbsR
4,AbsN,AbsN
```

diy_data > genotype_map.csv

```
treatment,sampleid,roi,gtype
fluc,tray2,0,wt
fluc,tray2,1,stn7
fluc,tray2,2,stn7
fluc,tray2,3,wt
```

Image processing and Output Visualization

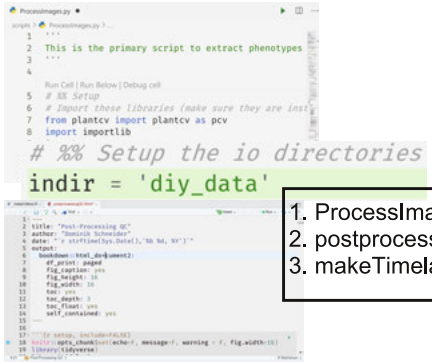

```
This is the primary script to extract phenotypes
# %% Setup the io directories
indir = 'diy_data'
```

1. ProcessImages.py
2. postprocessingQC.Rmd
3. makeTimelapse.R

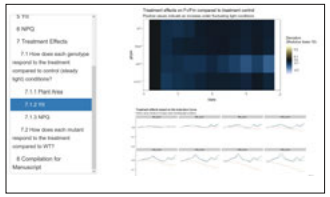

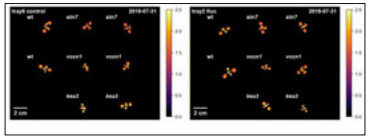

Figure 6

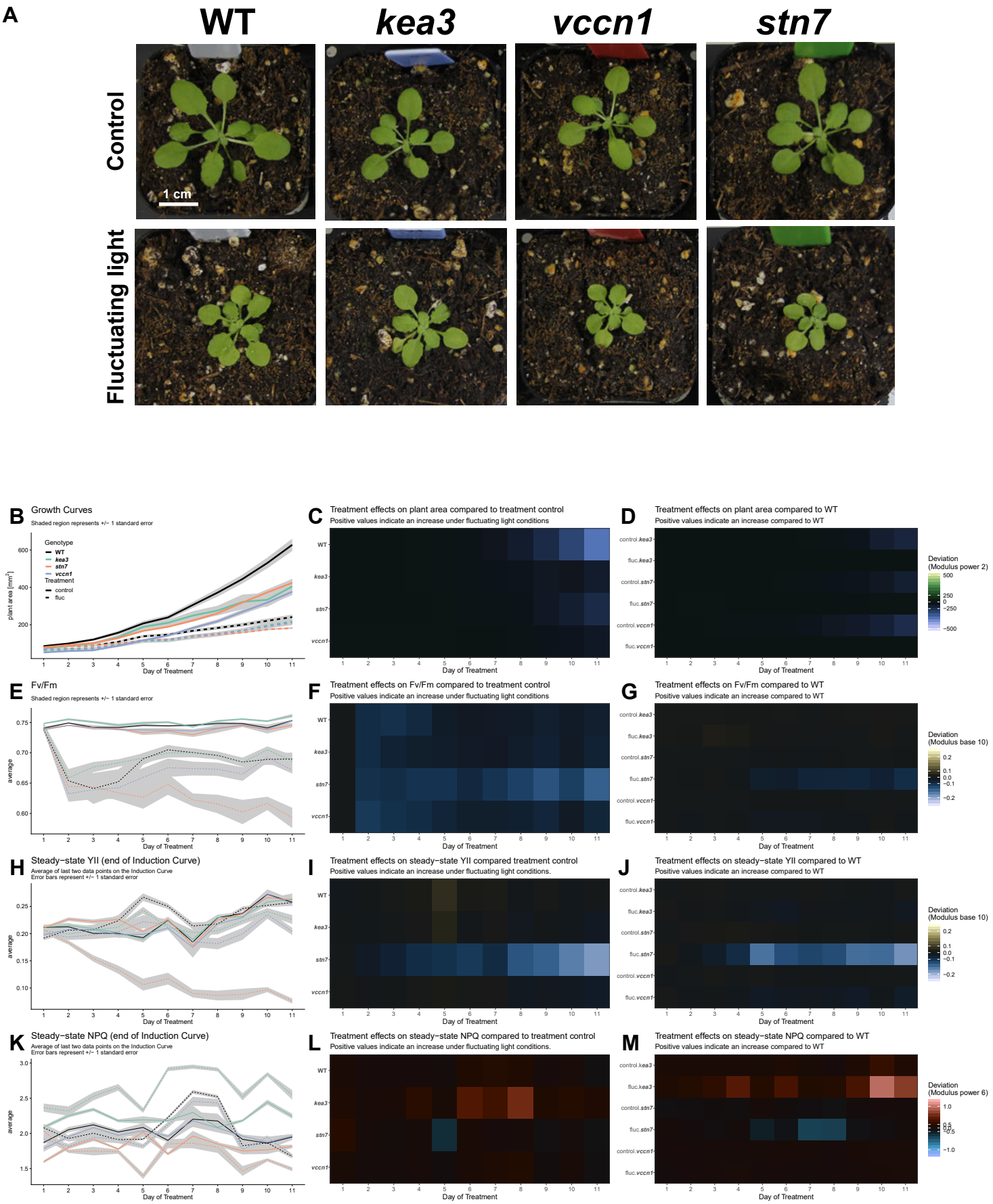
A
WT
kea3
vccn1
stn7
Control
Fluctuating light
1 cm
B
Growth Curves
Shaded region represents +/− 1 standard error
Genotype
WT
kea3
stn7
vccn1
Treatment
control
fluc
plant area [mm²]
Day of Treatment
C
Treatment effects on plant area compared to treatment control
Positive values indicate an increase under fluctuating light conditions
D
Treatment effects on plant area compared to WT
Positive values indicate an increase compared to WT
Deviation (Modulus power 2)
E
Fv/Fm
Shaded region represents +/− 1 standard error
average
F
Treatment effects on Fv/Fm compared to treatment control
Positive values indicate an increase under fluctuating light conditions
G
Treatment effects on Fv/Fm compared to WT
Positive values indicate an increase compared to WT
Deviation (Modulus base 10)
H
Steady−state YII (end of Induction Curve)
Average of last two data points on the Induction Curve
Error bars represent +/− 1 standard error
I
Treatment effects on steady−state YII compared treatment control
Positive values indicate an increase under fluctuating light conditions.
J
Treatment effects on steady−state YII compared to WT
Positive values indicate an increase compared to WT
K
Steady−state NPQ (end of Induction Curve)
Average of last two data points on the Induction Curve
Error bars represent +/− 1 standard error
L
Treatment effects on steady−state NPQ compared to treatment control
Positive values indicate an increase under fluctuating light conditions.
M
Treatment effects on steady−state NPQ compared to WT
Positive values indicate an increase compared to WT
Deviation (Modulus power 6)